Noise Effects on a Proposed Algorithm for Signal Reconstruction and Bandwidth Optimization

Original Scientific Paper

Ahmed F. Ashour
Electrical and Computer Engineering Department,
Idaho State University
921 S 8th Ave 83201, Pocatello, USA
ahmedashour@isu.edu

Ashraf A. M. Khalaf
Department of Electronics and Communications Engineering,
Faculty of Engineering, Department of Computer Science, Minia University
Damaris 61519, El-Minia, Egypt
ashraf.khalaf@mu.edu.eg

Aziza I. Hussein
Electrical and Computer Engineering Department,
Effat University
Al-Nazlah Al-Yamaniyah 34689, Jeddah, KSA
azibrahim@effatuniversity.edu.sa

Hesham F. A. Hamed
Faculty of Engineering, Egyptian Russian University
Faculty of Engineering, Minia University
Badr 11829, Cairo, Egypt
Damaris 61519, El-Minia, Egypt
hesham.fathy@eru.edu.eg

Ashraf Ramadan
Electrical and Computer Engineering Department,
Higher Technological Institute
Industrial Area2 44629, 10th of Ramadan, Egypt
ashraf.ramadan@hti.edu.eg

Abstract *– The development of wireless technology in recent years has increased the demand for channel resources within a limited spectrum. The system's performance can be improved through bandwidth optimization, as the spectrum is a scarce resource. To reconstruct the signal, given incomplete knowledge about the original signal, signal reconstruction algorithms are needed. In this paper, we propose a new scheme for reducing the effect of adding additive white Gaussian noise (AWGN) using a noise reject filter (NRF) on a previously discussed algorithm for baseband signal transmission and reconstruction that can reconstruct most of the signal's energy without any need to send most of the signal's concentrated power like the conventional methods, thus achieving bandwidth optimization. The proposed scheme for noise reduction was tested for a pulse signal and stream of pulses with different rates (2, 4, 6, and 8 Mbps) and showed good reconstruction performance in terms of the normalized mean squared error (NMSE) and achieved an average enhancement of around 48%. The proposed schemes for signal reconstruction and noise reduction can be applied to different applications, such as ultra-wideband (UWB) communications, radio frequency identification (RFID) systems, mobile communication networks, and radar systems.*

Keywords*: signal reconstruction, bandwidth optimization, AWGN, noise reduction, baseband signal, NMSE, noise reject filter*

1. INTRODUCTION

Every day, current analog signals like our voices are used in the real world. These signals need to be sampled, quantized, and encoded before being processed in a digital format [1]. "Reconstruction" or "interpolation" of the signal refers to the process of returning the sampled signal to its original analog form. Every one of our everyday devices undergoes the reconstruction process, which is crucial for restoring the signal to its original form [2]. Multiple schemes have been proposed for reconstructing a bandlimited signal from irregularly spaced sampling data [3-5]. The phase of the signal can be used for reconstructing the signal [6], and other schemes can be used without using it [7].

There are multiple research studies that have developed various strategies for reconstructing pulse and stream of pulse signals and used them in various systems. A proposed effective doppler-based signal reconstruc-

tion technique is used to restore the doppler spectrum in synthetic aperture radar (SAR) [8]. Other schemes based on compressed sensing (CS) are used for reconstructing the electrocardiogram (ECG) pulse signals [9-11], while [12] suggested a deep learning (DL)-based CS technique to reconstruct the ultrawideband (UWB) signal. Another approach is presented to the fast and accurate nonlinear pulse signal reconstruction for electromagnetic (EM) sensors and its applications [13]. Other algorithms are used for reconstructing variable-width pulses [14] and ultrashort pulses using DL [15]. The reconstruction of a stream of pulses for ultrasonic imaging was proposed using a noiseless finite rate innovation (FRI) method [16,17]. Many low-pass reconstruction problems have been successfully resolved via extrapolation [18-20].

In such real-world scenarios, it is necessary to establish appropriately accurate estimates of the inverse Fourier transform (IFT) based on this imperfect knowledge. The primary objective of the prior proposed work in [21] is to present a new method for extrapolating a finite-frequency segment of a time-limited baseband pulse signal. The approach relies on choosing a starting and ending frequency (f_s and f_e) to send through the bandlimited channel while utilizing a selective bandpass filter (BPF). A suggested algorithm is provided and put into practice on the receiver side in order to reconstruct the signal once more and recover the majority of the signal's energy. By adjusting the adaptive bandreject filter (BRF) in the receiver to only select the same transmitted band limits from f_s to f_e to reconstruct the signal, we can optimize the use of the channel bandwidth instead of selecting the entire signal spectrum or the main lobe band that contains the majority of the signal's power, as required by conventional methods. The results of the proposed algorithm showed that the algorithm converges when the number of iterations of the reconstruction algorithm is increased, as in the case of working with a noiseless channel.

This paper extends the work in [22] by studying the effect of additive white Gaussian noise (AWGN) on our previously proposed baseband signal transmission and reconstruction scheme and proposing a new technique to minimize the effect of noise using an adaptive noise reject filter (NRF), which consists of a bandpass filter (BPF) with the same starting and ending frequency parameters as the whole system. The proposed technique has been tested on a pulse and a stream of pulses and showed good reconstruction performance in terms of the normalized mean square error (NMSE) when compared to a noise-free channel. A list of used abbreviations is shown in Table 1.

The paper is organized as follows: Section 2 introduces the signal transmission and reconstruction scheme proposed previously and applied to a pulse and stream of pulses. Section 3 discusses the traditional and proposed solutions for reducing the noise added to the channel, their limitations, and the proposed applications of the scheme. Finally, Section 4 presents the conclusion.

Table 1. List of abbreviations

Abbreviation	Meaning
6G	sixth generation
AWGN	additive white Gaussian noise
BPF	bandpass filter
BPF	band-pass filter
BRF	band-reject filter
CS	compressed sensing
DFT	discrete fourier transform
DL	deep learning
dMRI	diffusion magnetic resonance imaging
DSIC	digital self-interference cancellation
DWT	discrete wavelet transform
ECG	electrocardiogram
EM	electromagnetic
EVVM	error vector magnitude
FFT	fast Fourier transform
FRI	finite rate innovation
FT	Fourier transform
IFT	inverse Fourier transform
IoT	internet of things
KPCA	kernel principal component analysis
LPF	low-pass filter
LPR	lost pulse ratio
LS	least squares
MSE	mean squared error
NMSE	normalized mean square error
NRF	noise reject filter
OFDM	orthogonal frequency division multiplexing
PSNR	peak signal-to-noise ratio
RFID	radio frequency identification
SAR	synthetic aperture radar
SI	self-interference
SPR	spurious pulse ratio
SVD	singular value decomposition
UHF	ultra-high frequency
UWB	ultrawideband
UWOC	underwater optical wireless communication
V2V	vehicle-to-vehicle communications
WSN	wireless sensor network

2. BASEBAND SIGNAL TRANSMISSION AND RECONSTRUCTION SCHEME

2.1 INTRODUCTION

The two main signal transmission mechanisms in any communication system are baseband and bandpass transmission. The baseband signal is distinguished by its low-frequency components, which include the DC component, such as the signal of the information source, such as human speech. Modulating the baseband signal to higher frequencies results in a bandpass signal. The resultant bandpass signal is concentrated around the carrier frequency, $\pm f_c$. Figs. 1(a) and (b) show examples of baseband signals such as a pulse signal $x_p(t)$ with a duration of 2 ms and a stream of pulses $x_{S8}(t)$ with a data rate of 8 Mbps.

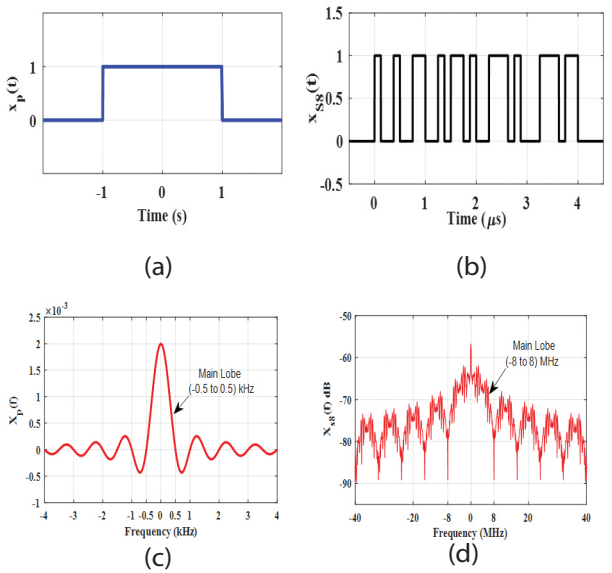

Fig. 1. Baseband signals (a) A pulse signal $x_p(t)$ with T=2 ms (b) A pulse stream $x_{S8}(t)$ with R_b= 8 Mbps (c) The spectrum of $x_p(t)$ (d) The spectrum of $x_{S8}(t)$

The Fourier transform (FT) can be used to obtain the amplitude spectra of $x_p(t)$ and $x_{S8}(t)$, as shown in Figs. 1(c) and (d), respectively. The figures show that the maximum power of these signals is concentrated around the zero frequencies in the main lobe (more than 90%), and the remaining power of the signals is distributed along the side lobes. Theoretically, these signals have infinite bandwidth and cannot be transmitted over band-limited channels. So, in order to send these signals over band limited channels, a low-pass filter (LPF) is applied to limit the signals' bandwidth and then transmitted over those channels as in conventional systems.

2.2. THE TRANSMISSION TECHNIQUE

Fig. 2 depicts the block diagram of the proposed technique for transmitting and reconstructing baseband signals. The transmitter consists of a generator to generate the baseband information $x(t)$, which is a pulse or stream of pulses in our study. The transmission technique depends on selecting any window (W) of the baseband signal using an adaptive BPF instead of sending the whole signal's spectrum or the main lobe only. The boundaries of the BPF are defined by a starting frequency f_s and an ending frequency f_e. The filter will produce a signal $g(t)$, which is distorted due to losing some of the signal's spectral information.

At the transmitter, assume that the selective BPF is adjusted to send a window (0.3-3) kHz from the original pulse's spectrum $x_p(f)$, which represents 17.2% of its total average power. Also, assume that the transmitted window of the pulse stream $x_{S8}(f)$ is (0.3-8.3) MHz, which represents 47.1% of its total average power.

Then, the transmitted signals $g_p(t)$ and $g_{S8}(t)$ will seem to be distorted due to losing some energy from their spectra, as shown in Fig. 3.

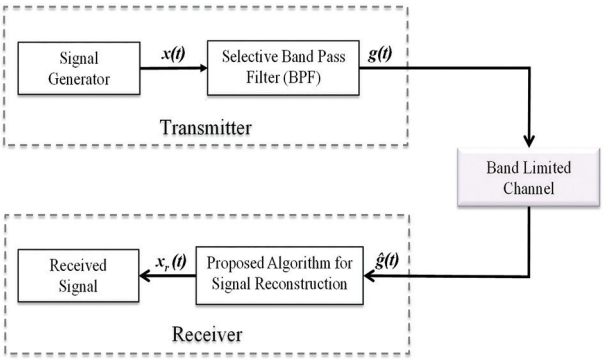

Fig. 2. Proposed technique's block diagram

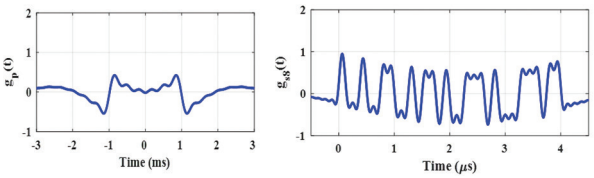

Fig. 3. Transmitted distorted signals of (a) $x_p(t)$ with W= (0.3-3) kHz (b) $x_{S8}(t)$ with W= (0.3-8.3) MHz

2.3. THE RECONSTRUCTION ALGORITHM

The block diagram of the baseband signal reconstruction algorithm at the receiver is shown in Fig. 4. The aim of this algorithm is to reconstruct the signal $x_r(t)$ with the knowledge of a segment $G(f)$ of the main signal's spectrum $X(f)$, then extrapolate the original signal's spectrum by making use of the received segment $\hat{G}(f)$, and a prior knowledge about the time extent of the transmitted signal.

The steps for reconstructing the baseband signal, as explained in Fig. 4, are as follows:

Step (1): IFT of the received signal's spectrum. The output is a non-time-limited signal.

Step (2): Multiplying by a gate (rect) function $p(t)$ with the same time extent as the original signal results in $s(t)$.

Step (3): Applying the FT to $s(t)$ to obtain $S(f)$, a non-bandlimited signal.

Step (4): Applying $S(f)$ to a BRF with the same starting and ending frequencies of the transmitter (f_s and f_e) to obtain $C(f)$.

Step (5): Adding the spectrum $C(f)$ with the known received signal's spectrum to be inserted into its dead space to be raised gives the first estimate of the reconstructed signal's spectrum $X_1(f)$.

Step (6): Calculating the IFT of $X_1(f)$ and repeating the loop again until reaching the required shape of the spectrum after N iterations.

Step (7): Calculating the IFT of $X_N(f)$ to get $x_n(t)$, which is the reconstructed signal after a certain number of iterations. The reconstructed baseband pulse stream signal of $x_{S8}(t)$ and its spectrum after 1 and 300 iterations are shown in Fig. 5.

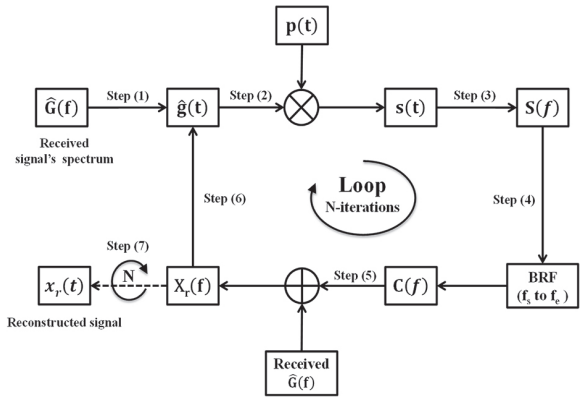

Fig. 4. The block diagram of baseband signal reconstruction algorithm

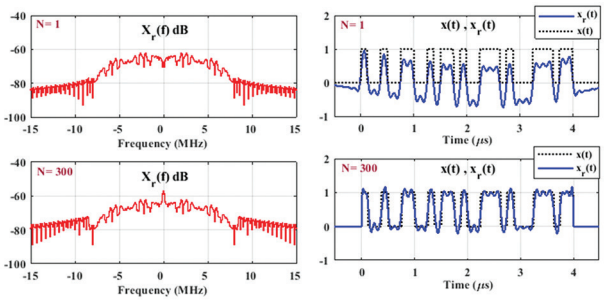

Fig. 5. The reconstructed pulse stream signal (8 Mbps) and its spectrum after 1 and 3000 iterations

3. RESULTS AND DISCUSSIONS

3.1. THE EFFECT OF AWGN ON THE ALGORITHM

In this section, the effect of adding the AWGN to the received signal will be determined, and the algorithm's behavior on the reconstructed signal will be checked. It is assumed that the transmitted pulse g(t) with a transmitted window band (0.3-3) kHz is passed through an AWGN with a SNR of 10 dB. The signal with noise $\hat{g}_n(t)$ in Fig. 6 (a) is received and applied to the proposed algorithm in Fig. 4 to reconstruct the baseband pulse signal again. As seen in Figs. 6 (b), (c), and (d), increasing N results in increasing the noise in the reconstructed signal. This is due to the accumulated addition of the received signal spectrum with noise $\hat{G}_n(f)$ in step 5 of the proposed algorithm shown in Fig. 4. So, the noise effect is increased by increasing the number of iterations; thus, the algorithm diverges.

Table 2 presents the impact of changing three key parameters – transmitted window bandwidth (W), number of iterations (N), and signal-to-noise ratio (SNR) – on the reconstruction status in the presence of AWGN.

Each column represents the variation of a single parameter, while the other parameters are held constant. The first column demonstrates the effect of altering the transmitted window bandwidth while keeping N and SNR fixed. Increasing W leads to a decrease in NMSE, indicating an improvement in the reconstruction's performance. The second column illustrates the effect of adjusting N while keeping W and NMSE constant. Here, we observe that increasing the number of iterations can result in a higher NMSE value, which suggests a negative impact on the reconstruction accuracy. The last column shows the effect of modifying SNR while keeping NMSE and N constant. It is evident that raising the SNR can lower the NMSE value, thereby improving the reconstruction performance. Therefore, an optimal balance between these parameters can be struck to meet the desired NMSE as per the system specifications.

Table 2. Effect of Transmitted Window Bandwidth, Number of Iterations, and SNR on Reconstruction Performance in the Presence of AWGN

Window BW (W) (N= 5, SNR=25 dB)		Variable (N) (W= 0-4 MHz, SNR= 25 dB)		Variable (SNR) (W= 0-4 MHz, N= 5)	
P %	NMSE	N	NMSE	SNR	NMSE
W= (0-2) MHz 86.94	0.1389	5	0.0868	15 dB	0.3518
W= (0-4) MHz 93.09	0.0903	10	0.1701	20 dB	0.1516
W= (0-6) MHz 95.46	0.0665	15	0.3180	25 dB	0.0863
W= (0-8) MHz 96.48	0.0576	20	0.4714	30 dB	0.0689

So, the traditional solutions to overcome the effect of noise in traditional systems are to increase the SNR at the receiver to overcome the noise signal's power, or to increase the transmitted window band. Although these solutions may work, we will propose another effective solution to reduce the effect of noise without any need to increase the SNR at the receiver or increase the transmitted window band.

3.2. THE PROPOSED NOISE REDUCTION SCHEME

As seen in the previous sub-section, adding the AWGN to the signal causes the algorithm to act very badly, and the signal cannot be reconstructed because the noise increases with every iteration, as shown in Fig. 6, causing the reconstructed signal to be loaded with more and more noise. The block diagram of the proposed technique to reduce the noise effect on our algorithm is shown in Fig. 7. The signals that explain the proposed scheme are shown in Fig. 8.

The steps of the proposed technique are as follows:

Step 1: Calculating the FT of the received signal with noise $\hat{g}_n(t)$ to get $\hat{G}_n(f)$ as shown in Fig. 8 (a) and (b).

Step 2: Applying $\hat{G}_n(f)$ to a NRF, which consists of a BPF with the same f_s and f_e as the transmitter and the receiver, in order to reject all the noise that exists along the signal's spectrum and keep the remaining spectrum as it is to result in a less noisy signal spectrum $\hat{G}(f)$ with zero noise in the shown regions (A, B, and C) in Fig. 8(c).

Steps (3-8): Applying the resultant spectrum of step 2 [$\hat{G}(f)$] to our proposed algorithm for N iterations, such as steps (1-6) in Fig. 4, to get XN(f).

Step 9: Calculating the IFT of XN(*f*) to get the reconstructed signal $x_r(t)$ after noise reduction, as shown in Fig. 8(d).

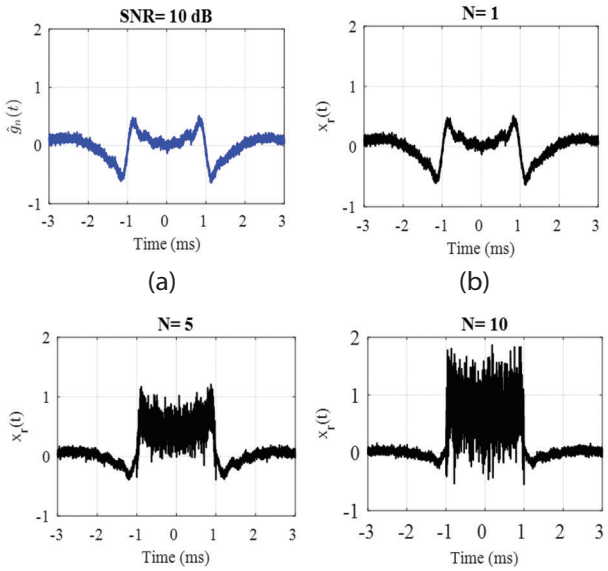

Fig. 6. Effect of increasing *N* in the presence of AWGN with SNR= 10 dB on the reconstructed pulse after (1, 5, and 10) iterations with a transmitted window band (0.3-3) kHz

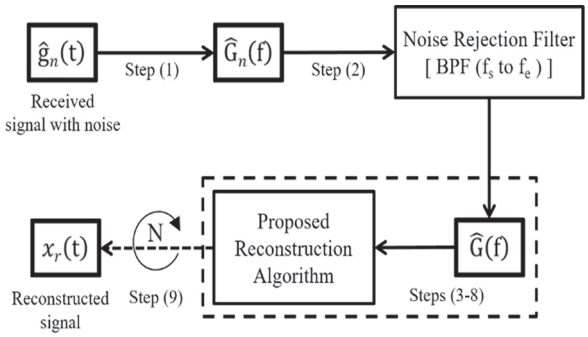

Fig. 7. Proposed noise reduction scheme block diagram

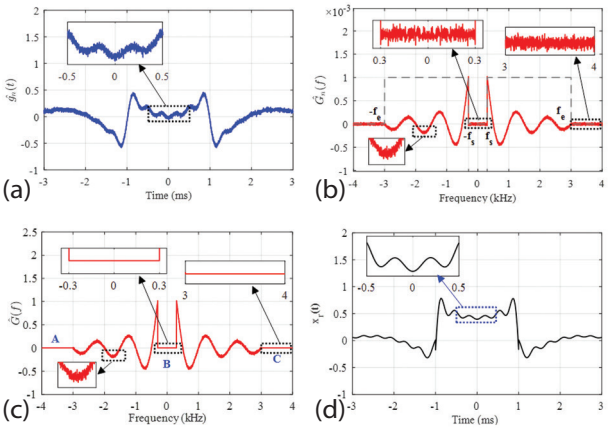

Fig. 8. Proposed noise reduction scheme signals: (a) Received signal with noise (b) FT of the received signal with noise (c) Received signal spectrum after noise reduction (d) Reconstructed signal after 5 iterations.

The proposed noise reduction technique is applied to different streams of pulses with different data rates, but we will focus on the results at 8 Mbps to be brief. Fig. 9 shows the reconstruction signals and their spectra in a noise-free channel and an AWGN for an 8 Mbps data rate with a transmitted window band (0.3-8.3) MHz, which contains ≈47% of the total signal's average power at SNR = 10 dB.

The Fig. 8 shows the reconstructed signal with accumulated noise after 5 iterations. The middle figure shows the reconstructed stream in a noiseless channel after applying the proposed noise reduction technique. It shows a good reconstruction status of the noisy signal after applying the scheme, which is very similar to the signal that is constructed without the existence of noise. A comparison of the spectra of all these signals is shown in the figure below. Also, the spectra of the reconstructed signals with and without noise are almost identical.

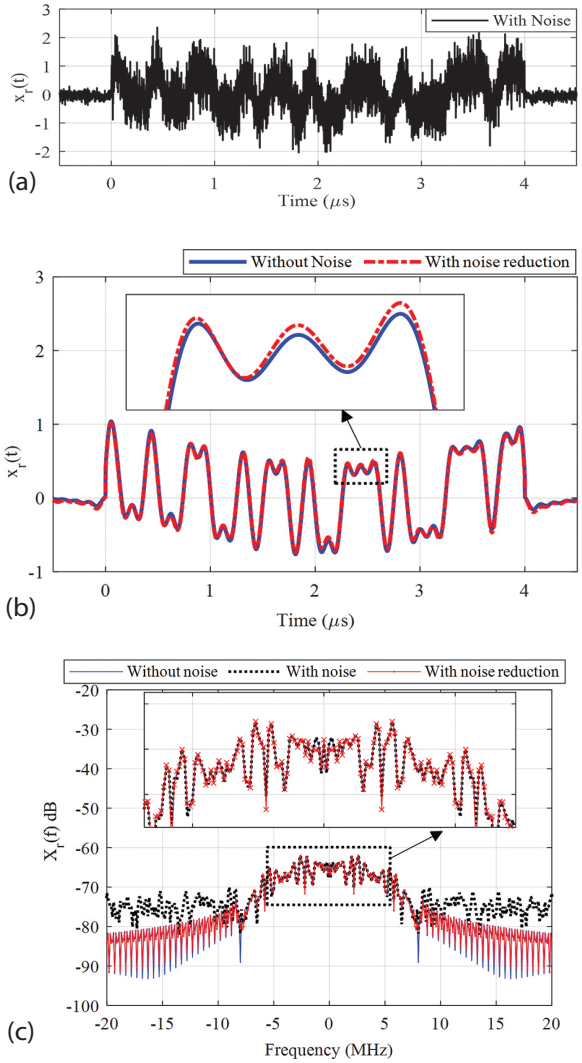

Fig. 9. Effect of noise reduction scheme on a transmitted window (0.3-8.3) MHz of an 8 Mbps stream with SNR = 10 dB, N =5 (a) Reconstructed signal without noise reduction (b) Reconstructed signal with noise reduction (c) A comparison of reconstructed signals' spectra

A comparison between the NMSE of the reconstructed stream of pulses in a noise-free channel and the AWGN channel after noise reduction with the same parameters as in the previous section for different SNRs is shown in Fig. 10. For example, let us compare the reconstructed signal without noise and with 10 dB AWGN. Their NMSEs at different iterations are recorded in Table 3 for comparison. The figure also shows that when N<200 for any SNR value, the reconstructed signal after reducing the noise has a better reconstruction status than the reconstructed signal when the channel is noiseless, as it has a better NMSE value of 0.0719 than the other one (0.1256). This is approved in Fig. 11(a), as the mid-level amplitude of $x_r(t)$ with noise reduction has the same mid-level amplitude of the original signal $x(t)$, but $x_r(t)$ without noise has a shifted value (0.24) by ≈50% from $x(t)$.

At N= 184, there is an intersection between the two NMSE curves at 0.0723, in which the mid-level amplitudes of the reconstructed signals in both cases have an amplitude offset of 20% away from $x(t)$, as shown in Fig. 11(b). At N = 300, $x_r(t)$ without noise has a better performance than the other one (with noise), as it has a lower NMSE value (0.0556) and has the same mid-level amplitude value of $x(t)$ as seen in Fig. 11(c). So, it is recommended to use the proposed technique for noise reduction to reconstruct an 8 Mbps stream signal in a noisy channel at N = 100 or 150.

The effect of changing both N and SNR on the reconstructed signal after applying the noise reduction technique in the presence of the AWGN channel is shown in Fig. 12. It depicts that increasing N results in enhancing the NMSE value for any SNR. But fixing N while increasing the SNR value does not enhance the NMSE very well except at low SNR values (≤5 dB). So if the designer needs to improve the reconstruction performance using the proposed noise reduction scheme, he/she does not need to increase the signal's power, but he/she should increase the number of iterations to achieve a good reconstruction status.

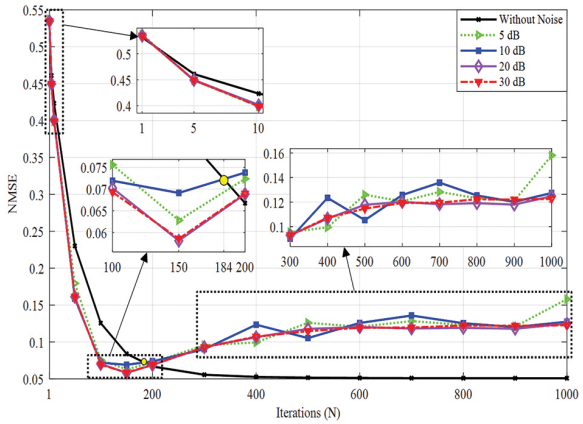

Fig. 10. A Comparison between the NMSE of the reconstructed 8 Mbps stream of pulses with a transmitted window (0.3-8.3) MHz without and with the addition of AWGN in different SNRs

Table 3. NMSE of the reconstructed 8 Mbps stream in noise-free and AWGN channels at different iterations

Reconstructed signal $x_r(t)$	NMSE at SNR= 10 dB		
	N = 100	N = 184	N = 300
Without noise	0.1256	0.0723	0.0556
With noise reduction	**0.0719**	**0.0723**	0.0902

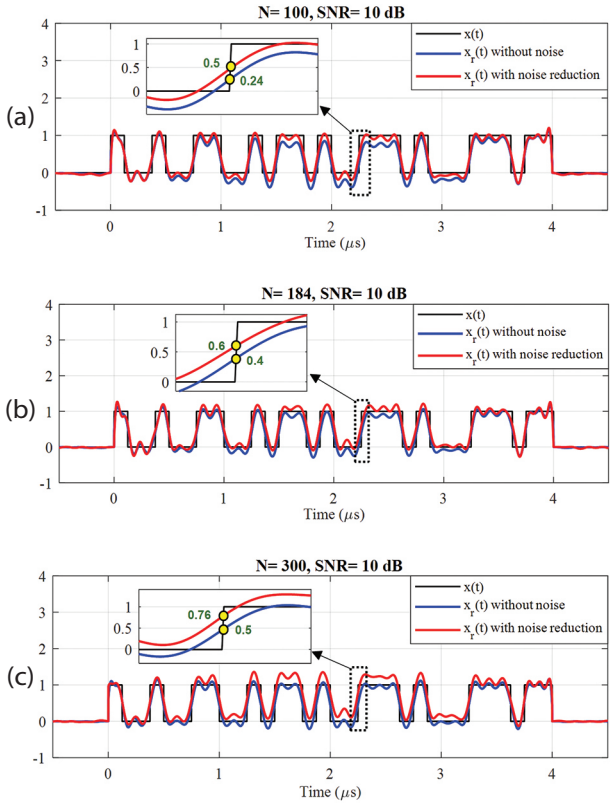

Fig. 11. A comparison between the generated 8 Mbps stream with the reconstructed streams in noise-free channel and AWGN channel at SNR= 10 dB when (a) N= 100, (b) N= 184, and (c) N= 300.

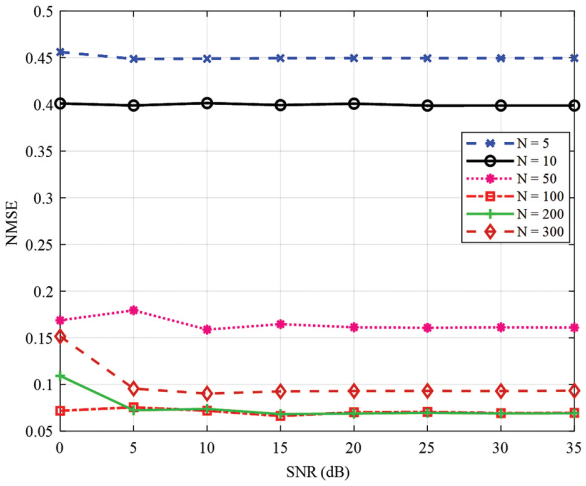

Fig. 12. Effect of changing the SNR on the reconstruction algorithm in the presence of AWGN for the same data in Fig. 9 for different iterations

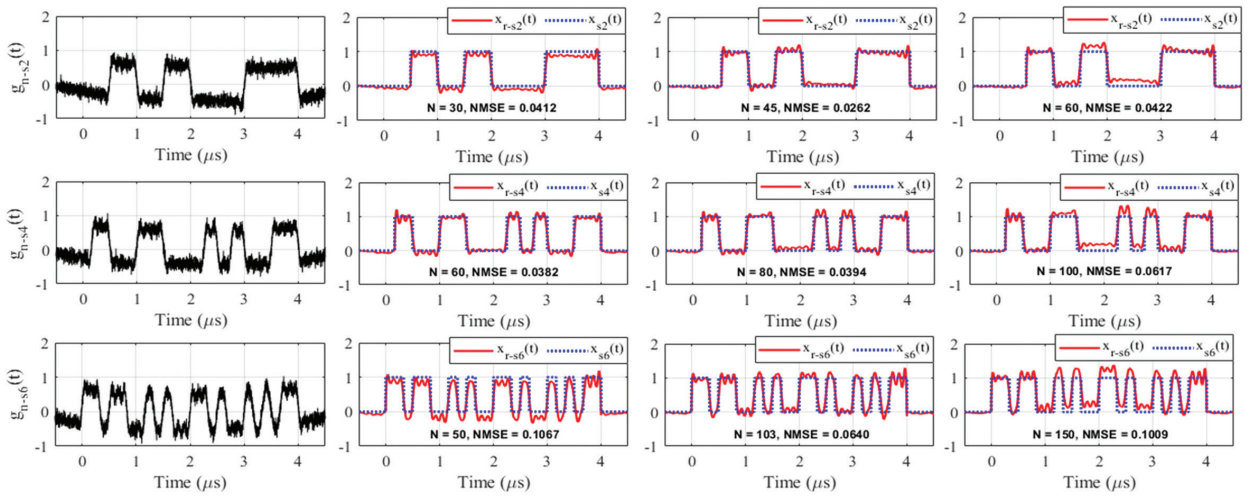

Fig. 13. Reconstructed 2, 4, and 6 Mbps data streams with noise at SNR= 10 dB, W= 0.3-8.3 MHz and different iterations

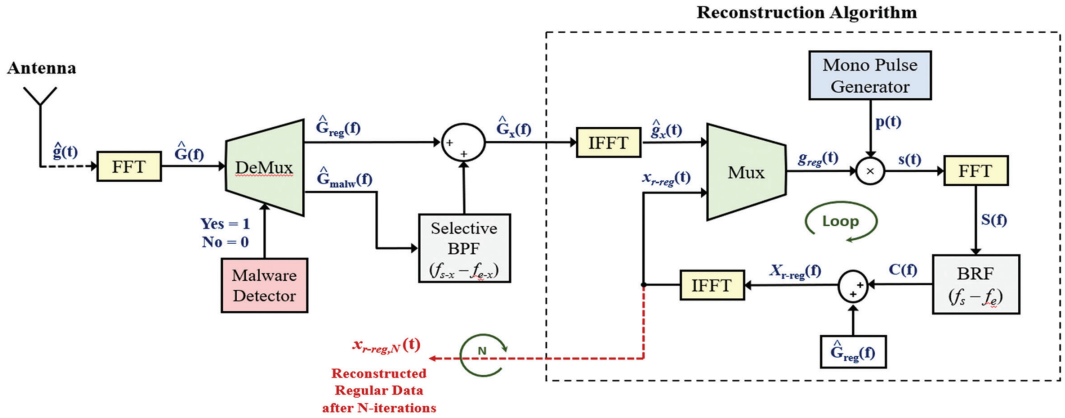

Fig. 14. The proposed reconstruction algorithm in the RFID reader

Table 4. Comparison of Signal Reconstruction and Noise Reduction Techniques for Various Noisy Systems and Applications

Ref. (Year)	Signal Type	System/ Application	Reconstruction Algorithm	Noise Type	Noise Reduction Technique	Performance Metrics & Result
[23] (2020)	Stream of pulses	IoT and mobile WSN	Sparse pulse representation for signal reconstruction	AWGN	Using denoising autoencoders	- Proposed method: LPR = 0.01, SPR = 0.02 - Conventional method: LPR = 0.05, SPR = 0.1
[24] (2021)	OFDM	IBFD communication in OFDM-based wireless systems	DSIC techniques, for estimating the SI channel and reconstruction of the SI signal	CP noise	CPNR	- Improved total suppression by 6 db. - Improved EVM by 5%
[25] (2022)	ECG pulses	Portable heartbeat detection system	DWT	AWGN	A combination of DWT and SVD	Proposed method average: MSE = 0.002, PSNR = 60.5 dB
[26] (2022)	Stream of pulses	X-ray single-particle imaging	A neural network pipeline for restoring diffraction intensities.	Poisson noise	Poisson noise reduction	An improvement in the MSE of roughly two orders of magnitude.
[27] (2021)	dMRI signal	MRI based systems	KPCA	AWGN	KPCA denoising	Better SNR improvements up to 2.7x
[28] (2022)	OFDM	UWOC systems	CS- based channel estimation	AWGN	Setting a noise threshold to remove useless channel taps.	Increased NMSE by 67% and 97% than and 97% than DFT and LS algorithms respectively
Proposed Method (2023)	Stream of pulses	Baseband and speech signals	Proposed Baseband signal reconstruction algorithm	AWGN	NRF	An improved average NMSE by 47.7% after 100 iterations

Figure 13 depicts the implementation of the proposed noise reduction scheme for reconstructing baseband signals from random streams of pulses with different data rates (2, 4, and 6 Mbps), transmitted window bandwidth of 0.3–8.3 MHz, and varying numbers of iterations, at an SNR of 10 dB. The received stream signals with noise for the different data rates are denoted by $g_{n\text{-}sx}(t)$, while $x_{r\text{-}sx}(t)$ and $x_{sx}(t)$ represent the reconstructed and original generated signals, respectively, which are compared to each other in each subfigure. The figure clearly illustrates the successful application of our proposed noise rejection scheme to reconstructing different data streams. The NMSE initially decreases as the number of iterations (N) increases but reaches a certain value beyond which it diverges and results in a worse NMSE value. For example, signal reconstruction for the 2 Mbps stream is perfect when the algorithm is run for up to 45 iterations, but beyond this point, the NMSE increases, leading to bad signal reconstruction status. Similarly, the optimal number of iterations for the 4 Mbps and 6 Mbps streams are 50 and 103, respectively. It is worth noting that our noise reduction scheme using the NRF has limitations in that it cannot be applied for any number of iterations, as it converges to a certain number of iterations and then diverges.

Table 4 shows a comparison between different signal reconstruction and noise reduction schemes and their state-of-the-art applications. Their evaluation metrics are also compared in terms of lost pulse ratio (LPR), spurious pulse ratio (SPR), mean squared error (MSE), NMSE, and peak signal-to-noise ratio (PSNR). In [23], the authors propose a denoising autoencoder-based sparse pulse representation method for internet of things (IoT) and mobile wireless sensor network (WSN) systems where the proposed method achieved lower values of LPR and SPR compared to the conventional method. In [24], the authors use different digital self-interference cancellation (DSIC) techniques for self-interference (SI) channel estimation and reconstruction in orthogonal frequency division multiplexing (OFDM)-based wireless systems. The proposed DSIC technique resulted in a 6 dB improvement in total suppression and a 5% improvement in error vector magnitude (EVM). In [25], the authors combine discrete wavelet transform (DWT) and singular value decomposition (SVD) for ECG pulse denoising in a portable heartbeat detection system. The proposed method achieved an improved MSE of 0.002 and a PSNR of 60.5 dB.

In [26], a neural network pipeline for restoring diffraction intensities in X-ray single-particle imaging systems affected by Poisson noise is proposed, and this method resulted in an improvement in the MSE of roughly two orders of magnitude. The authors in [27] apply kernel principal component analysis (KPCA) denoising to diffusion magnetic resonance imaging (dMRI) signals in MRI-based systems. The proposed KPCA approach led to better SNR improvements of up to 2.7x. In [28], the authors employ a compressed sensing (CS)-based channel estimation technique and set a noise threshold to remove useless channel taps in underwater optical wireless communication (UWOC) systems affected by AWGN. The proposed approach outperformed discrete fourier transform (DFT) and least squares (LS) algorithms in terms of NMSE by 67% and 97%, respectively. Finally, the proposed approach applies a baseband signal reconstruction algorithm to AWGN in stream of pulses, baseband, and speech signals, achieving an improved average NMSE by 47.7% after 100 iterations.

3.3. PROPOSED APPLICATIONS

In [22], the proposed baseband signal reconstruction algorithm was applied to different signal types such as pulse, triangular, composite, analog, stream of pulses, and speech signals, and the algorithm showed its success in reconstructing most of their signals' energy and thus reconstructing them. The proposed scheme for baseband signal reconstruction can be used in various applications to reconstruct signals. For example, in UWB communications, it can reconstruct short-width pulses, while in radio frequency identification (RFID) systems, it can extract data transmitted by tags. Additionally, it can optimize bandwidth in mobile communication systems and recover pulses in radar systems. It can also optimize bandwidth in speech and audio processing applications.

In [29], a proposed real-world application in ultra-high frequency (UHF) RFID systems in which the proposed algorithm is used to reconstruct the bit stream of regular data in malware-free and malware-injected scenarios, as shown in Fig. 14. In a malware-free scenario, the received signal g(t) is fed to a fast Fourier transform (FFT) block and then identified as malware-free or malware-injected data by the malware detector block. If it is malware-free, the data is passed directly to the reconstruction algorithm to recover the original regular data, but if it is malicious, it extracts the missing spectrum of the original regular data from the malicious data spectrum and then adds it to the received regular data spectrum, and then the proposed reconstruction algorithm is applied to recover the regular data more quickly.

4. CONCLUSION AND FUTURE WORK

This paper proposes a noise reduction scheme to minimize the effect of noise on a proposed algorithm used to reconstruct the baseband signals. The algorithm is based on sending small-transmitted window that carries a portion of the original signal's energy, and then reconstructing the signal again, thus optimizing the used channel bandwidth. Although the algorithm converges in noise-free channels, it diverges when noise is present, leading to bad reconstruction status in each iteration of the algorithm. At the receiver, the noise can be minimized by using a traditional way by compromising between three parameters, the transmitted window bandwidth, the number of iterations and SNR, but this is not an effective solution. So,

a noise reduction scheme based on adaptive NRF is proposed which is a function of the system's starting and ending frequencies. When tested on a baseband pulse and a stream of pulses in the presence of AWGN, the suggested scheme showed good reconstruction performance in reducing the noise effect. The performance was evaluated in terms of NMSE compared to free noise channels. It was applied to different streams of pulses with various data rates (2, 4, 6, and 8 Mbps) and demonstrated good reconstruction performance in terms of NMSE, but only up to a certain number of iterations, after which the proposed scheme diverged. This algorithm may find applications in future sixth generation (6G) wireless networks, UWB communications, radar systems, RFID-based systems, and vehicle-to-vehicle communications (V2V). Future research can further study this algorithm in these cases.

5. REFERENCES

[1] M. M. Richter, S. Paul, V. Këpuska, M. Silaghi. "Digital Signal Representation", In Signal Processing and Machine Learning with Applications, Springer, 2022, pp. 3-38.

[2] Y. Yamamoto, M. Nagahara, P. P. Khargonekar, "A brief overview of signal reconstruction via sampled-data H∞ optimization", Applied and Computational Mathematics, Vol. 11, No. 1, 2012, pp. 3-18.

[3] L. Guo, C. W. Kok, H. C. So, W. S. Tam, "Fast and L2-optimal recovery for periodic nonuniformly sampled bandlimited signal", Signal Processing, Vol. 180, 2021, p. 107856.

[4] Z.-C. Zhang, "Nonuniform reconstruction of periodic bandlimited signals without sampling points' number restriction", Optik, Vol. 207, 2020, p. 163798.

[5] H. Zhao, R. Wang, D. Song, "Recovery of Bandlimited Signals in Linear Canonical Transform Domain from Noisy Samples", Circuits, Systems, and Signal Processing, Vol. 33, No. 6, Jan. 2014, pp. 1997-2008.

[6] V. Kishore, S. Mukherjee, C. S. Seelamantula, "Phase Sense—Signal Reconstruction from Phase-Only Measurements via Quadratic Programming", Proceedings of the International Conference on Signal Processing and Communications, Bangalore, India, 19-24 July 2020, pp. 1-5.

[7] R. Balan, B. G. Bodmann, P. G. Casazza, D. Edidin, "Fast algorithms for signal reconstruction without phase", SPIE Proceedings, Vol. 6701, 2007.

[8] S.-S. Zuo, M. Xing, X.-G. Xia, G.-C. Sun, "Improved Signal Reconstruction Algorithm for Multichannel SAR Based on the Doppler Spectrum Estimation", IEEE Journal of Selected Topics in Applied Earth Observations and Remote Sensing, Vol. 10, No. 4, 2017, pp. 1425-1442.

[9] J. Chen, S. Sun, N. Bao, Z. Zhu, L. -B. Zhang, "Improved Reconstruction for CS-Based ECG Acquisition in Internet of Medical Things", IEEE Sensors Journal, Vol. 21, No. 22, 2021, pp. 25222-25233.

[10] Z. Zhang et al. "Electrocardiogram Reconstruction Based on Compressed Sensing", IEEE Access, Vol. 7, 2019, pp. 37228-37237.

[11] M. Al Disi et al. "ECG Signal Reconstruction on the IoT-Gateway and Efficacy of Compressive Sensing Under Real-Time Constraints", IEEE Access, Vol. 6, 2018, pp. 69130-69140.

[12] Z. Luo, J. Liang, J. Ren, "Deep Learning Based Compressive Sensing for UWB Signal Reconstruction", IEEE Transactions on Geoscience and Remote Sensing, Vol. 60, 2022, pp. 1-10.

[13] K. Abratkiewicz, P. Samczyński, "A Block Method Using the Chirp Rate Estimation for NLFM Radar Pulse Reconstruction", Sensors, Vol. 19, No. 22, Nov. 2019, p. 5015.

[14] G. Baechler, A. Scholefield, L. Baboulaz, M. Vetterli, "Sampling and Exact Reconstruction of Pulses with Variable Width", IEEE Transactions on Signal Processing, Vol. 65, No. 10, 2017, pp. 2629-2644.

[15] T. Zahavy, A. Dikopoltsev, O. Cohen, S. Mannor, M. Segev, "Deep Learning Reconstruction of Ultrashort Pulses", Optica, Vol. 5, No. 5, 2018, pp. 666-673.

[16] G. Baechler, A. Scholefield, L. Baboulaz, M. Vetterli, "Sampling and Exact Reconstruction of Pulses with Variable Width", IEEE Transactions on Signal Processing, Vol. 65, No. 10, May 2017, pp. 2629-2644.

[17] A. G. J. Besson, "Imaging from Echoes: On Inverse Problems in Ultrasound", École Polytechnique Fédérale de Lausanne, Switzerland, PhD Thesis, 2019.

[18] S. Xu, S. Tao, Y. Chai, X. Yang, Y. He, "The extrapolation of bandlimited signals in the offset linear canonical transform domain", Optik, Vol. 180, 2019, pp. 626-634.

[19] J. Weng, "A new one-step band-limited extrapolation procedure using empirical orthogonal functions", Journal of Electronics, Vol. 23, No. 5, 2006, pp. 777-780.

[20] M. Milman, "Extrapolation and optimal decompositions: with applications to analysis", Springer-Verlag, 1994.

[21] A. F. Ashour, A. Khalaf, A. Hussein, H. Hamed, A. Ramadan, "A New Algorithm for Baseband Pulse Transmission over Band-Limited Channels for Wireless Automotive Communications", International Journal of Advanced Trends in Computer Science and Engineering, Vol. 9, No. 4, 2020, pp. 5222-5228.

[22] A. F. Ashour, A. Khalaf, A. Hussein, H. Hamed, A. Ramadan, "A Proposed Signal Reconstruction Algorithm over Bandlimited Channels for Wireless Communications", Advances in Electrical and Computer Engineering, Vol. 23, No. 1, 2023, pp. 19-32.

[23] X. Li, Z. Liu, Z. Huang. "Deinterleaving of pulse streams with denoising autoencoders", IEEE transactions on aerospace and electronic systems, Vol. 56, No. 6, 2020, pp. 4767-4778.

[24] H. Ayar, O. Gurbuz, "Cyclic prefix noise reduction for digital self interference cancellation in OFDM-based in-band full-duplex wireless systems", IEEE Transactions on Wireless Communications 20, No. 9, 2021, pp. 6224-6238.

[25] G. Huang, Z. Yang, W. Lu, H. Peng, J. Wang, "Sub-Nyquist sampling of ECG signals based on the extension of variable pulsewidth model", IEEE Transactions on Instrumentation and Measurement, Vol. 71, 2022, pp. 1-14.

[26] A. Bellisario, F. R. N. C. Maia, T. Ekeberg. "Noise reduction and mask removal neural network for X-ray single-particle imaging", Journal of Applied Crystallography, Vol. 55, No. 1, 2022, pp. 122-132.

[27] G. Ramos-Llordén et al. "SNR-enhanced diffusion MRI with structure-preserving low-rank denoising in reproducing kernel Hilbert spaces", Magnetic Resonance in Medicine 86, No. 3, 2021, pp. 1614-1632.

[28] X. Liu, J. Hu, K. Zhang, X. Tang, Y. Dong, "On Channel Estimation Based on Compressed Sensing for OFDM UWOC Systems", Proceedings of the Asia Communications and Photonics Conference, Shenzhen, China, 5-8 November 2022, pp. 1039-1042.

[29] A. F. Ashour, C. Condie, C. Pocock, S. C. Chiu, A. Chrysler, M. M. Fouda, "A Spectrum Injection-Based Approach for Reconstructing Regular Data from Malware-Injected Data in UHF RFID Systems", Proceedings of the IEEE Global Communications Conference, 2023. (in press)